ENVIRONMENTAL RESEARCH LETTERS

LETTER • OPEN ACCESS

A surface temperature dipole pattern between Eurasia and North America triggered by the Barents–Kara sea-ice retreat in boreal winter

To cite this article: Yurong Hou *et al* 2022 *Environ. Res. Lett.* **17** 114047

ENVIRONMENTAL RESEARCH
LETTERS

CrossMark

OPEN ACCESS

RECEIVED
19 August 2022

REVISED
9 October 2022

ACCEPTED FOR PUBLICATION
31 October 2022

PUBLISHED
11 November 2022

LETTER

A surface temperature dipole pattern between Eurasia and North America triggered by the Barents–Kara sea-ice retreat in boreal winter

Yurong Hou[1,2], Wenju Cai[3,4,5], David M Holland[6], Xiao Cheng[7], Jiankai Zhang[8], Lin Wang[1], Nathaniel C Johnson[9], Fei Xie[10], Weijun Sun[11], Yao Yao[1], Xi Liang[12], Yun Yang[10], Chueh-Hsin Chang[13], Meijiao Xin[1,2] and Xichen Li[1,*]

1 Institute of Atmospheric Physics, Chinese Academy of Sciences, Beijing, People's Republic of China
2 University of Chinese Academy of Sciences, Beijing, People's Republic of China
3 Frontiers Science Center for Deep Ocean Multispheres and Earth System and Physical Oceanography Laboratory, Ocean University of China, Qingdao, People's Republic of China
4 Qingdao National Laboratory for Marine Science and Technology, Qingdao, People's Republic of China
5 Centre for Southern Hemisphere Oceans Research (CSHOR), CSIRO Oceans and Atmosphere, Hobart, TAS, Australia
6 Courant Institute of Mathematical Sciences, New York University, NY, United States of America
7 School of Geospatial Engineering and Science, Sun Yat-sen University, Zhuhai, People's Republic of China
8 Key Laboratory for Semi-Arid Climate Change of the Ministry of Education, College of Atmospheric Sciences, Lanzhou University, Lanzhou, People's Republic of China
9 NOAA/Geophysical Fluid Dynamics Laboratory, Princeton, NJ, United States of America
10 College of Global Change and Earth System Science, Beijing Normal University, Beijing, People's Republic of China
11 College of Geography and Environment, Shandong Normal University, Jinan, People's Republic of China
12 Key Laboratory of Research on Marine Hazards Forecasting, National Marine Environmental Forecasting Center, Beijing, People's Republic of China
13 Department of Atmospheric Sciences, National Taiwan University, Taipei, Taiwan
* Author to whom any correspondence should be addressed.

E-mail: lixichen@mail.iap.ac.cn

Keywords: Barents–Kara sea ice, land-area surface air temperature, dipole pattern, Arctic amplification

Supplementary material for this article is available online

Abstract

The Arctic has experienced dramatic climate changes, characterized by rapid surface warming and sea-ice loss over the past four decades, with broad implications for climate variability over remote regions. Some studies report that Arctic warming may simultaneously induce a widespread cooling over Eurasia and frequent cold events over North America, especially during boreal winter. In contrast, other studies suggest a seesaw pattern of extreme temperature events with cold weather over East Asia accompanied by warm weather in North America on sub-seasonal time scales. It is unclear whether a systematic linkage in surface air temperature (SAT) exists between the two continents, let alone their interaction with Arctic sea ice. Here, we reveal a dipole pattern of SAT in boreal winter featuring a cooling (warming) in the Eurasian continent accompanied by a warming (cooling) in the North American continent, which is induced by an anomalous Barents–Kara sea-ice decline (increase). The dipole operates on interannual and multidecadal time scales. We find that an anomalous sea-ice loss over the Barents–Kara Seas triggers a wavenumber one atmospheric circulation pattern over the high-latitude Northern Hemisphere, with an anomalous high-pressure center over Siberia and an anomalous low-pressure center over high-latitude North America. The circulation adjustment generates the dipole temperature pattern through thermal advection. Our finding has important implications for Northern Hemisphere climate variability, extreme weather events, and their prediction and projection.

1. Introduction

Since the 1970s, climate change over the Northern Hemisphere high latitudes has intensified compared to those of the global mean, as a result of a process known as Arctic amplification [1, 2]. The most significant changes occurred in boreal autumn and winter [3], characterized by a rapid surface air temperature (SAT) increase, more than twice as fast as the global warming rate [2], accompanied by a continuous sea-ice retreat [4–7]. These rapid Arctic changes have been associated with a series of physical processes [8, 9], including the local anthropogenic greenhouse gas forcing [10, 11], the lapse rate and Planck feedbacks [12, 13] in the atmosphere, as well as the cloud feedbacks [14, 15], the ice albedo-feedback [16], and tropical-polar teleconnections [17]. In particular, the ocean-atmosphere heat exchange induced by the recent Arctic sea-ice loss [18] and the heat and moisture transport between the Arctic and lower latitudes [19, 20] play a crucial role in heating the North Pole region, especially during boreal winter when the shortwave radiative forcing is absent over the Arctic region.

Arctic Amplification has a broad implication on climate changes and variability over the mid- and high-latitude Northern Hemisphere, especially over the continental areas [21–23]. The warm Arctic, associated with the sea ice melt, and the rapid increase of Eurasian snow cover [24–26] in boreal autumn and winter, are often followed by a decrease in SAT over the mid-latitude Eurasian continent [27, 28], and sometimes over the mid-latitude North American continent [29] in boreal winter. This pattern has been termed the 'warm Arctic—cold continent' pattern which includes cooling in eastern North America [24, 26]. Hypotheses proposed to explain mechanisms associated with this pattern include: stratospheric–tropospheric coupling induced by an enhanced upward propagation of planetary-scale waves with wavenumbers of one and two [30, 31], a weakening of the Arctic Oscillation [32], a persistent shift of Arctic polar vortex towards the Eurasian continent [33], and more frequent Eurasian blocking events associated with an intensified Siberian High [34, 35]. These mechanisms are in part triggered by the Arctic sea-ice retreat, especially over the Barents–Kara Seas (BKS) region.

Several recent studies questioned the significance level of the impacts of the Arctic sea-ice loss on the Northern Hemisphere mid-latitude climate in boreal winter [7, 36–38]. Large discrepancies exist between the observations and numerical simulations, as well as among the experiments results using different numerical models [7]. Some modeling studies based on large ensembles [39–43] indicated that the observed cold anomaly over the Eurasian continent may be more attributed to the atmospheric internal variability and the forcing from the tropics, rather than driven by the Arctic sea-ice loss. Other studies indicated that the atmospheric response to the Arctic sea-ice loss may be underestimated in climate models [44, 45] in comparison to that in the observations. In addition, the linkage between the Arctic and the mid-latitudes is weakening according to a recent study [46].

The sea-ice loss and the circulation changes over different sectors of the Arctic Ocean may have distinct impacts on mid-latitude North America [47]. The surface warming and the sea-ice loss over the Chukchi–Bering Seas usually drive an anomalous cooling over North America [29]. In addition, the weakening of stratospheric polar vortex [48–50] associated with the Arctic sea-ice loss can cause the increase of the extreme cold events over North America [51, 52], other studies [53, 54] revealed a seesaw pattern of extreme temperature events on subseasonal time scales, with a cold event over East Asia accompanied by a warm event in North America, usually lasting for several weeks [54]. Despite the weak cooling temperature trend in February, there has been a warming trend in wintertime monthly-mean SAT over North America during the past decades [55, 56], which contravenes the hypothesis that a warm Arctic is associated with a cold North America.

This study reveals a 'cold Eurasia-warm North America' SAT dipole pattern between the mid-latitude Eurasian continent and much of North America in boreal winter (December–January–February, DJF), active on interannual and multidecadal time scales triggered by BKS sea-ice variability. In particular, the BKS sea-ice loss, while cooling the Eurasian continent, instead heats the North American continent through atmospheric circulation adjustment and its associated thermal advection.

2. Materials and methods

2.1. Data analysis

The UK Met Office Hadley Centre's sea surface temperature (SST) and sea-ice datasets [57] have been used in this study to estimate variability and trends of the Arctic sea ice concentration (SIC) and SST. Sea level pressure (SLP) and SAT from the three reanalysis datasets are also used. To estimate the continental dipole pattern and its relationship with the anomalous Arctic sea ice and atmospheric circulation over Northern Hemisphere in boreal winter (DJF), we use (a) the Modern Era Retrospective-Analysis for Research and Applications, version 2 (MERRA2) [58]; (b) the European Centre for Medium-Range Weather Forecasts Reanalysis version 5 (ERA5) [59]; and (c) the Japanese 55 year Reanalysis (JRA55) [60]. To estimate the multidecadal trend of the SAT, we use a two-meter air temperature (T2m) of 10 252 land-based weather stations from the National Center for

Environmental Information, National Oceanic and Atmospheric Administration [61].

2.2. Statistical methods

Sen's slope method [62] is used to calculate the observed trends in SAT and the Arctic SIC, with the confidence intervals estimated using the Mann-Kendall test [62].

We use the linear regression coefficients to evaluate the relationship between the temperature, the atmospheric circulation, and the sea ice. We use the Student's t-test to calculate the confidence intervals of these coefficients.

We use empirical orthogonal function (EOF) [63] to obtain the leading modes of SAT over the Northern Hemispheric mid-latitude continents, focusing on boreal winter (DJF). The EOF decomposition is applied based on both trend-retained and detrended reanalysis datasets. The results of these two types of decomposition are identical in this study.

A maximized covariance analysis (MCA) method [64] is used to retrieve the most important coherent modes between Arctic sea ice and SAT over Northern Hemispheric continents to determine the linkage between these two variables. The leading modes of MCA maximize the covariance between two high-dimensional datasets through a singular value decomposition of the covariance matrix between these two variables. This method gives the most important modes that dominate the variability of each time series, and shows a strong correlation with each other.

We use a dynamical adjustment (DA) method [65] to isolate anomalous atmospheric circulation modes associated with the evolution of the area-averaged SAT over mid-latitude Eurasia and North America. This method, based on partial least-squares regression and spatial pattern correlation, separates the SAT component associated with atmospheric circulation. Based on the above two procedures, SLP modes that significantly contribute to the area-averaged SAT time series are obtained. Cross-validation with a bootstrap method is used to evaluate whether the contribution of these modes is statistically significant.

2.3. Model simulation

The NCAR climate model, the Community Atmosphere Model version 5 (CAM5), is used to investigate the teleconnection between the Arctic sea-ice and the continental SAT and SLP. We employ the finite-volume dynamical core with a global horizontal resolution of about 2° (F19). The Community Land Model and the Community Sea-Ice Model thermodynamic module provide the heat and moisture fluxes on the lower boundary. A transient experiment with CAM5 forced by observed time-varying (with trend) SST and sea ice (i.e. AMIP-like) is performed for the 1979–2019 period, with 20 ensemble members accompanied by different perturbed initial conditions. The experiment is forced by the SST and sea ice variability over the BKS region (0°–80° E, 65° N–80° N). The SST and SIC over other areas are set to the climatological mean states (1981–2010) with the annual cycle, while other forcings, including the concentration of greenhouse gases, the aerosols, and the solar radiation, are all set to fixed values during the entire integration period. The linear trend of the ensemble mean state from 1980 to 2019 is calculated, which represents the impact of the SST and sea ice over the BKS region on the changes of the Northern Hemispheric SAT and SLP.

3. Results

3.1. Dipole pattern on interannual time scales

We identify leading modes of interannual SAT variability of boreal winter (DJF) from 1980 to 2019 by performing an EOF decomposition (see section 2.2) over the entire continental area of the mid-latitude Northern Hemisphere (20° N–70° N) with three state-of-the-art reanalysis datasets, the MERRA2 (see supplementary figures 1(a) and (b)), the ERA5 (see supplementary figures 1(c) and (d)), and the JRA55 (see supplementary figures 1(e) and (f)). The results among different datasets are identical. The first EOF mode (see supplementary figures 1(a), (c) and (e)) shows a coherent warming pattern over almost the entire Eurasian and North American continents, except the areas around Hudson Bay and Greenland. This mid-latitude warming pattern is tightly associated with the anthropogenic global warming trend. Mode two (see supplementary figures 1(b), (d) and (f)) shows a dipole pattern between Eurasia and North America, with anomalous cooling over the Eurasian continent and a broad warming pattern over North America. The Eurasian cooling—North American warming pattern should be reversed when the principle component (PC) is negative. Mode one and two explain about 24% and 15% of the total variability, respectively. We also perform an EOF analysis with a linear trend removed before the decomposition, and the resulting patterns are identical (see supplementary figure 2).

To further investigate the potential linkage between the Arctic sea ice and the land-area SAT over the mid-latitude Northern Hemisphere, we conduct a Maximum Covariance Analysis (MCA) (see section 2.2) between these two variables in DJF. The spatial pattern of the SIC (figure 1(a)) of the leading MCA mode is characterized by sea-ice retreat over the BKS and the Greenland Sea. The spatial pattern of the SAT (figure 1(b)) resembles the second EOF mode of the SAT (see supplementary figure 1(b)), with a broad cooling pattern over mid-latitude Eurasia and continental-wide warming over entire North America, despite a cooling signal around the west coast of the United States. This SAT dipole pattern between the Eurasian and the North American

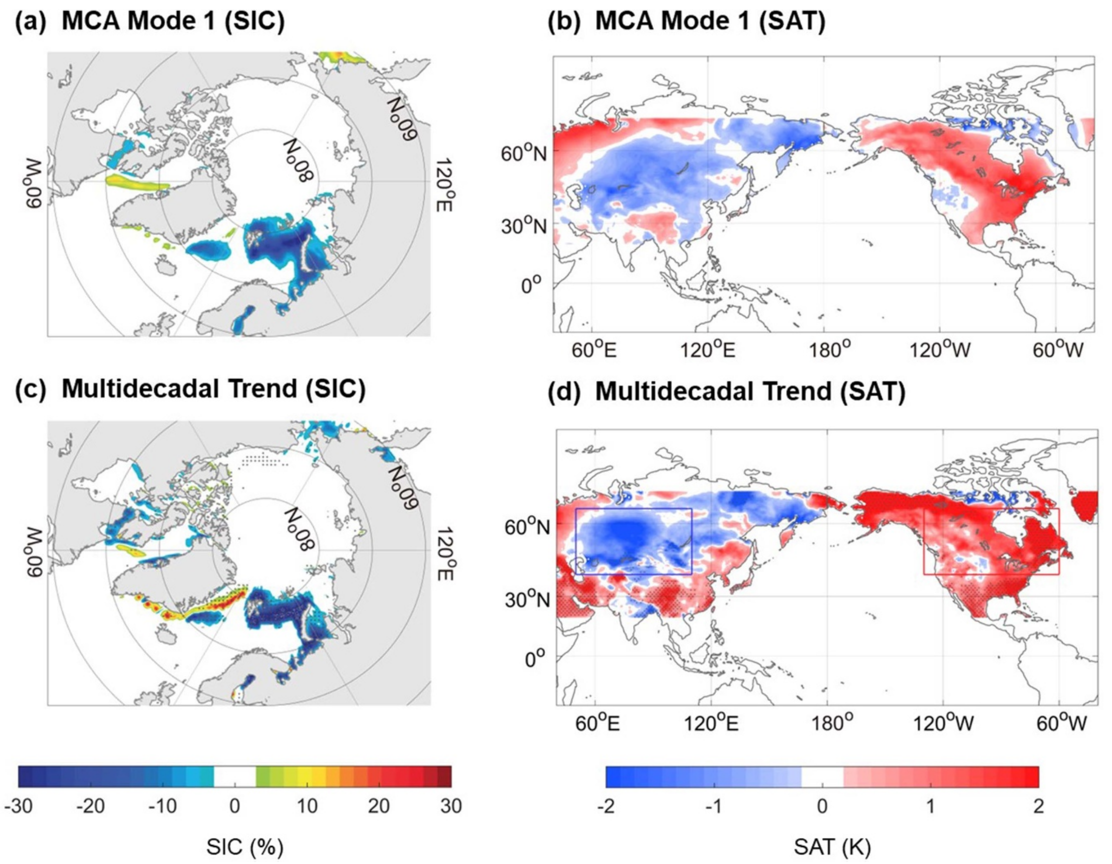

Figure 1. Observed evidence of a boreal winter dipole of cold Eurasia—warm North America. (a) and (b) show the first mode of a maximized covariance analysis (MCA) between the boreal winter (DJF) Arctic sea ice concentration (SIC, (a)) and the mid-latitude Northern Hemispheric land-area surface air temperature (SAT, (b)). (c) and (d) show observed DJF trends of the Arctic SIC ((c), % (40 yr)$^{-1}$) and the mid-latitude SAT ((d), K (40 yr)$^{-1}$) during the 1980–2019 period. Stippling indicates areas with a statistical significance level of <5% based on a Mann-Kendall test. The similarity between the MCA and linear trends of the SIC and SAT implies a robust, coherent SAT dipole pattern associated with the Barents–Kara SIC anomalies on interannual and multidecadal time scales.

continents may be reversed when the sea ice increases over the BKS. To confirm the relationship revealed by the decomposition, we also perform an MCA using detrended SIC and SAT (see supplementary figure 4). The second mode (see supplementary figures 4(c) and (d)) resembles the linkage between the BKS sea-ice retreat and the continental SAT dipole pattern. Using other reanalysis datasets produces nearly identical MCA results (see supplementary figure 6).

The EOF decomposition reveals a SAT dipole pattern between the Eurasian and North American continents, while the MCA links it to the variability of the Arctic SIC, especially that over the BKS and Greenland Sea. We then regress the SAT (figure 2(a)) onto the area-averaged BKS (20° E–80° E, 70° N–80° N) SIC time series (black curve in supplementary figure 3). The results are similar to the dipole-like SAT pattern (figure 1(b)) in the first MCA mode, confirming that this SAT dipole pattern is related to the BKS sea-ice variability.

Considering that the adjustment of the atmospheric circulation may play an important role in mediating these kinds of remote effects [66–68], we further regress the Northern Hemisphere SLP and the 500 hPa geopotential height (figure 2(b)) onto the area-weighted mean BKS SIC time series (black curve in supplementary figure 3). The result shows a wavenumber one pattern over the high-latitude Northern Hemisphere, with a high-pressure center over north Siberia, and a low-pressure center over the high-latitude North America. Further analysis (see supplementary figure 9) indicates that the large-scale circulation anomalies related to the BKS sea-ice retreat may intensify the cold advection over central Eurasia, meanwhile driving an anomalous warm advection to mid-latitude North America, contributing to the SAT dipole pattern between the two continents in boreal winter.

With a combination of statistical analyses, including EOF, MCA, and linear regression, we reveal that the Arctic sea-ice variability, especially over the BKS, may contribute to this SAT dipole pattern through modulating the atmospheric circulation over the mid- and high-latitude Northern Hemisphere. This phenomenon operates on interannual time scales. Below, we show that such a diploe pattern operates on multidecadal time scales.

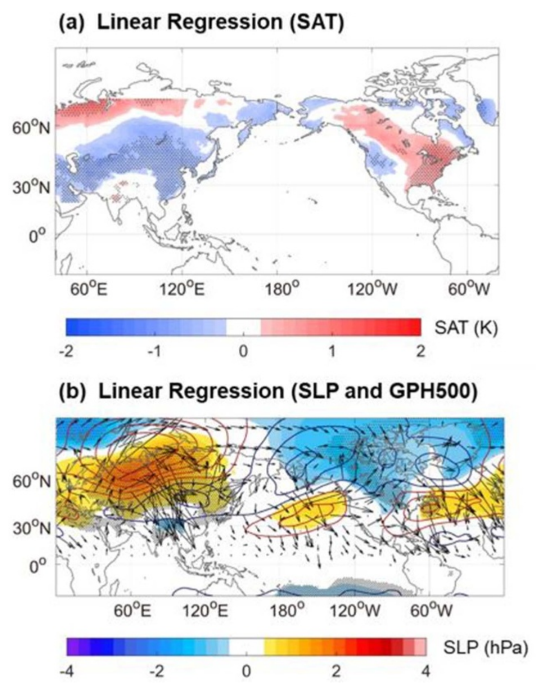

Figure 2. Surface air temperature and atmospheric circulation responses to the Barents–Kara sea-ice loss in boreal winter. (a) Pattern of linear regression coefficient of the mid-latitude Northern Hemisphere surface air temperature against standardized time series of the sea ice concentration (SIC) over the Barents–Kara Seas in boreal winter (DJF). (b) Patterns of regression coefficients of the sea level pressure (shaded), the 500 hPa geopotential height (contours at 6 m intervals), and the horizontal component of the Plumb flux at 500 hPa (vectors) against the standardized time series of the DJF Barents–Kara SIC. Stippling indicates areas with a statistical significance level of <5% based on Student's *t*-test.

3.2. Dipole pattern in multidecadal trend

We calculate the DJF SIC and SAT trends from 1980 to 2019. As revealed by many previous studies [7, 69–71], the wintertime Arctic sea ice experienced a rapid retreat over the BKS, and part of the Nordic—Greenland Seas (figure 1(c)), mainly due to the warm surface water intrusion associated with the shift of the Gulf stream extension [72, 73]. Central Eurasia experienced a cooling trend [28, 45, 74, 75]. In contrast, North America experienced a broad warming trend in boreal winter [55, 56, 76] (figure 1(d), based on the MERRA2 reanalysis), despite a spot of mild cooling over the Rocky Mountain area. We also calculate the mid-latitude Northern Hemisphere SAT trend using other reanalysis datasets (ERA5 and JRA55) and *in-situ* observations (see supplementary figure 8). Results show a similar dipole pattern, with a cooling signal over central Eurasia and a broad warming pattern over mid-latitude North America. However, the intensity of the temperature trends among these datasets varies.

To evaluate the potential trigger of these opposite SAT trends between the two continents, we perform a DA analysis (see section 2.2) to the area-weighted mean DJF SAT time series over the central Eurasian continent (40° N–65° N, 50° E–110° E, blue box in figure 1(d)) and the North American continent (40° N–65° N, 60° W–130° W, red box in figure 1(d)), respectively. The DA technique isolates the effects of dynamical processes on the SAT trends. The dynamical component is determined through the identification of atmospheric circulation patterns (e.g. anomalous high-/low-SLP centers) that impact the SAT through thermal advection [65].

Figures 3(a) and (b) show the anomalous SLP patterns, which significantly contribute to the recent observed SAT trends over central Eurasia (figure 3(a)) and North America (figure 3(b)), respectively through the DA. Our results indicate that both the negative SAT trend over central Eurasia and the positive SAT trend over North America can be at least partially attributed to a similar atmospheric circulation pattern (figures 3(a) and (b)). This pattern is characterized by a strong high-pressure center over north Siberia, and a relatively weaker low-pressure center over northern Canada and Hudson Bay. It constitutes a wavenumber one pattern over the northern high latitudes along with a high-pressure center over the North Pacific. The thermal advection associated with the high- and low-pressure centers helps advect cold and warm air to central Eurasia and North America, respectively, forming a SAT dipole pattern between these two continents in boreal winter.

According to the DA, the dipole-like SAT trend between the Eurasian and North American continents may be associated with a wavenumber one circulation pattern over the high-latitude Northern Hemisphere (figure 3). This pattern resembles the anomalous circulation pattern related to the BKS sea-ice retreat (figure 2(b)). This similarity implies that the BKS sea-ice loss may impact the Northern Hemispheric land-area SAT trend through an adjustment of the atmospheric circulation. Additional evidence is needed to validate the causality and to clarify the mechanisms of these linkages, which we provide below with numerical model experiment.

3.3. Causality and mechanism

We conduct an ensemble simulation experiment using the NCAR climate model, the Community Atmosphere Model version 5 (CAM5), driven by the observed evolution of the SST and SIC over the BKS region from 1980 to 2019 (see section 2.3). The simulation results provide the atmospheric temperature and circulation responses to the forcings from the Arctic (figure 4). The simulated SAT trend shows a similar dipole-like pattern, with cooling signals over central Eurasia and a broad, significant warming pattern over North America (figure 4(a)). However, the cooling signal is not strong in all regions. The high-latitude Eurasian continent is dominated by a strong warming, which agrees well with our MCA results. The impact of the Arctic sea ice on the Eurasian

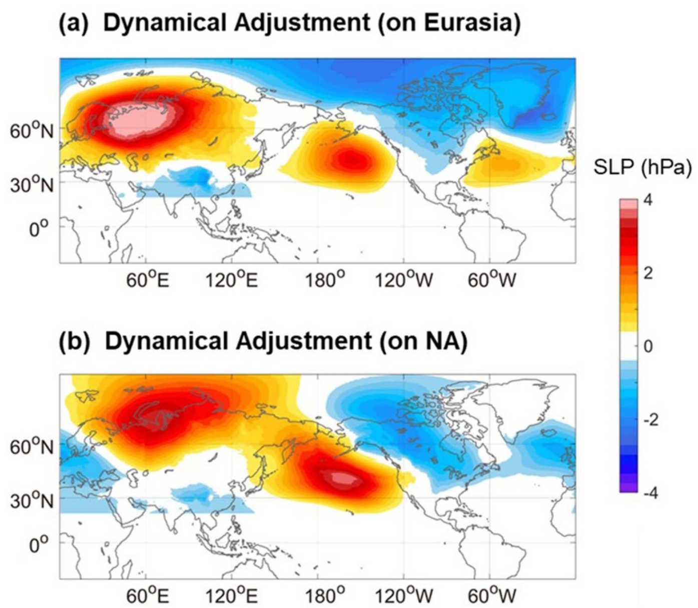

Figure 3. Atmospheric circulation associated with dipole pattern of mid-latitude surface air temperature. (a) Sea level pressure (SLP) pattern associated with the time series of the area-weighted mean surface air temperature (SAT) over central Eurasia (blue box in figure 1(d)) in boreal winter (DJF), retrieved by a dynamical adjustment (DA) analysis. (b) Same as (a), but for the SLP pattern associated with the area-averaged SAT time series over North America (NA, red box in figure 1(d)) based on the DA. A DA procedure separates the dynamical (associated with atmospheric circulation) and thermodynamical components from the SAT trend (see section 2.2).

cooling trend has been intensely investigated [27–29]. The robustness of this effect has been questioned [39–41, 45, 77, 78], as debate surrounding the uncertainties of the simulation results continues. Previous studies [28, 79, 80] indicated that simulating the impact of Arctic sea ice on the Eurasia cooling may need a large sample size due to the low signal-to-noise ratio. Remarkably, the relationship between the BKS sea-ice loss and the heating over North America, as revealed in this study, is significant in both the statistical analysis (figure 2(a)) and numerical simulation (figure 4), presenting a robust linkage between these processes.

The DA and linear regression analysis imply that the linkage between the Arctic sea-ice retreat and the SAT dipole pattern is likely mediated by atmospheric dynamics, mainly through a zonal wavenumber one mode over the northern high latitudes. A high-pressure center characterizes the circulation pattern over Siberia and a low-pressure center over North America, along with a high-pressure center over the mid-latitude North Pacific (figures 2(b) and 3), despite a slight deviation of the intensity among different high- and low-pressure centers. We further analyze the simulation results (figure 4(b)) to elucidate the circulation response to the BKS sea-ice retreat. The SLP response to the BKS SST/SIC (figure 4(b)) forcings reproduce a high-pressure center over Siberia and a low-pressure center over North America. However, the former is stronger in the simulation results than in the statistical analyses (figures 3 and 4). It extends to the east coast of the Eurasian continent and merges with a high-pressure center over the North Pacific. The low-pressure center in the simulation results is relatively weaker than that in the statistical analyses.

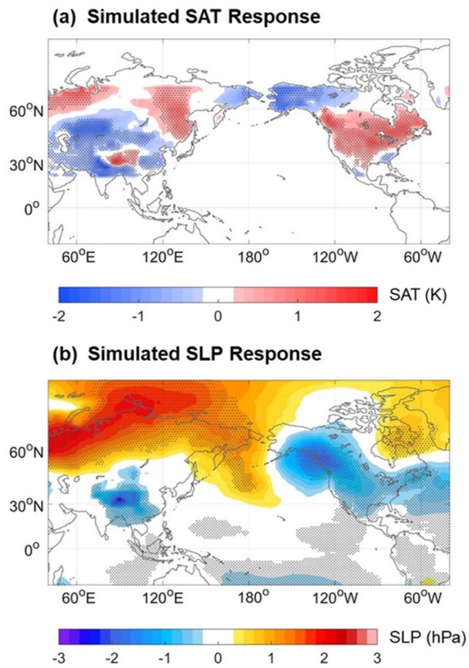

Figure 4. Simulated response to the observed Arctic SST and SIC. (a) The wintertime (DJF) SAT response (K (40 yr)$^{-1}$) to the SST and SIC variability over the Barents–Kara Seas (BKS) region during the 1980–2019 period. (b) The wintertime SLP response (hPa (40 yr)$^{-1}$) to SST and SIC variability over the BKS region during the 1980–2019 period. Stippling indicates areas with a statistical significance level of <5% based on a Mann-Kendall test.

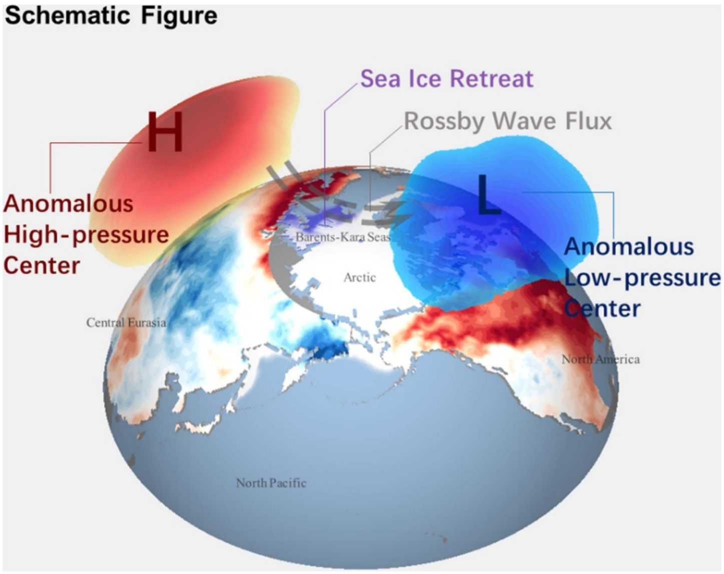

Figure 5. Schematic diagram of the mechanism for the Cold Eurasia—Warm North America pattern triggered by the sea-ice retreat over the Barents–Kara Seas in boreal winter. The sea-ice retreat over the Barents–Kara Seas heats the surface atmosphere and triggers an anomalous high-pressure center over northern Siberia, propagating to the east through stationary Rossby wave dynamics (with wavenumber one), forming an anomalous low-pressure center over high-latitude North America. The anomalous high-pressure center drives an anomalous cold atmospheric advection from the Arctic to central Eurasia. In contrast, the anomalous low-pressure center drives an anomalous warm advection to the central-east North American continent.

These circulation patterns in both statistical analyses and the numerical experiment are significant almost everywhere, which reemphasizes the role of the circulation patterns in mediating the Arctic sea-ice variability and the continental SAT dipole pattern. Recent studies indicated that the BKS sea-ice retreat might shift the stratospheric polar vortex to the Eurasian continents [33]. The BKS sea-ice retreat may also intensify the Siberian high or Ural blocking by heating the atmosphere, expanding the geopotential heights, and weakening the westerly wind [28, 35, 81]. This signal may propagate to the east through a stationary Rossby wave train, contributing to the formation of the low-pressure center over North America.

To examine the Rossby wave dynamics, we estimate the horizontal component of Plumb flux [82] at 500 hPa (vectors in figure 2(b)), which represents the direction and the intensity of the propagation of a Rossby wave train. Results show a clear wave flux from the Siberian High to the anomalous low-pressure center over North America, forming a wave number one pattern of the mid- to high-latitude Northern Hemisphere (figure 2(b)), agreeing well with our simulation results (figure 4(b)).

4. Conclusion and discussion

We reveal a continental dipole pattern of the SAT in boreal winter, with opposite temperature signals over central Eurasia and North America, operating in both the interannual variability and multidecadal trend of wintertime land-area SAT over the mid-latitude Northern Hemisphere. This pattern is seen in the EOF decomposition of both the trend-retained and detrended land-area SAT time series over the mid-latitude Northern Hemisphere. This dipole pattern in MCA and linear regression is linked to an Arctic sea-ice retreat, especially over the BKS region. We show that the BKS sea-ice retreat drives a wavenumber one atmospheric circulation pattern over the high-latitude Northern Hemisphere (figure 5). The circulation anomalies further advect cold and warm air to the Eurasian and North American continents (see supplementary figure 9) respectively, forming the SAT dipole pattern in boreal winter.

Our results indicate that the BKS sea-ice loss may contribute to the cooling over Eurasia during winter, agreeing well with previous studies [27, 28, 74]. On the other hand, we clarify that the BKS sea-ice loss also intensifies the warming trend over North America, although the impact of Arctic sea ice in different regions is different [47]. Recent studies show robust evidence [50, 52, 83] that the Arctic sea-ice variability may drive extreme cold events over both Asia and North America through stratospheric polar vortex disruption. Additional investigation is needed to determine to what extent Arctic sea-ice retreat-induced mean warming over North America is offset by the more frequent cold extreme events.

Eurasia and North America are two heavily populated continents. The dipole pattern we find may also influence the precipitation and air pollution with broad societal implications, including economic and public health consequences in these regions. The pattern potentially contributes to climate predictability on interannual and multidecadal time scales.

Data availability statement

The data that support the findings of this study are available upon reasonable request from the authors.

Acknowledgments

Yurong Hou, Wenju Cai, and Xichen Li are supported by the National Key Research and Development Program of China (2018YFA0605700). Yurong Hou and Xichen Li are supported by the National Natural Science Foundation of China (Grant Nos. 42176243, 41976193 and 41676190). Wenju Cai is funded by the Strategic Priority Research Program of the Chinese Academy of Sciences (Grant No. XDB40000000) and CSHOR, which is a joint research Centre for Southern Hemisphere Oceans Research between QNLM and CSIRO. David M Holland is funded by the Center for Global Sea Level Change (CSLC) of NYU Abu Dhabi Research Institute (G1204) in the UAE, NSF International Thwaites Glacier Collaboration MELT PLR-1739003 and NASA Oceans Melting Greenland (OMG) NNX15AD55G. Xiao Cheng is funded by the Innovation Group Project of Southern Marine Science and Engineering Guangdong Laboratory (Zhuhai) (Grant No. 311021008). Jiankai Zhang is supported by the Project for Longyuan Youth Innovation and Entrepreneurship Talent of Gansu. Nathaniel C Johnson bases funding from the National Oceanic and Atmospheric Administration to the Geophysical Fluid Dynamics Laboratory. Weijun Sun is funded by the National Natural Science Foundation of China (Grant No. 42271145). Yao Yao is supported by the National Natural Science Foundation of China (Grant Nos. 41975068 and 42150204). Yun Yang is supported by the National Natural Science Foundation of China (Grant No. 41976005). Chueh-Hsin Chang is supported by MOST 110-2111-M-002-015 from the Ministry of Science and Technology of Taiwan.

ORCID iDs

Lin Wang https://orcid.org/0000-0002-3557-1853
Fei Xie https://orcid.org/0000-0003-2891-3883
Yao Yao https://orcid.org/0000-0002-6425-7855
Chueh-Hsin Chang https://orcid.org/0000-0003-4558-9755
Xichen Li https://orcid.org/0000-0001-6325-6626

References

[1] Serreze M C and Barry R G 2011 Processes and impacts of Arctic amplification: a research synthesis *Glob. Planet. Change* **77** 85–96

[2] Cohen J, Screen J A, Furtado J C, Barlow M, Whittleston D, Coumou D, Francis J, Dethloff K, Entekhabi D and Overland J 2014 Recent Arctic amplification and extreme mid-latitude weather *Nat. Geosci.* **7** 627–37

[3] Screen J A and Simmonds I 2010 Increasing fall-winter energy loss from the Arctic Ocean and its role in Arctic temperature amplification *Geophys. Res. Lett.* **37** L16707

[4] Screen J A and Simmonds I 2010 The central role of diminishing sea ice in recent Arctic temperature amplification *Nature* **464** 1334–7

[5] Taylor P C, Cai M, Hu A, Meehl J, Washington W and Zhang G J 2013 A decomposition of feedback contributions to polar warming amplification *J. Clim.* **26** 7023–43

[6] Dai A, Luo D, Song M and Liu J 2019 Arctic amplification is caused by sea-ice loss under increasing CO_2 *Nat. Commun.* **10** 1–13

[7] Cohen J, Zhang X, Francis J, Jung T, Kwok R, Overland J, Ballinger T, Bhatt U, Chen H and Coumou D 2020 Divergent consensuses on Arctic amplification influence on midlatitude severe winter weather *Nat. Clim. Change* **10** 20–29

[8] Screen J A, Deser C and Simmonds I 2012 Local and remote controls on observed Arctic warming *Geophys. Res. Lett.* **39** L10709

[9] Park K, Kang S M, Kim D, Stuecker M F and Jin -F-F 2018 Contrasting local and remote impacts of surface heating on polar warming and amplification *J. Clim.* **31** 3155–66

[10] Alexeev V, Langen P and Bates J 2005 Polar amplification of surface warming on an aquaplanet in "ghost forcing" experiments without sea ice feedbacks *Clim. Dyn.* **24** 655–66

[11] Stuecker M F, Bitz C M, Armour K C, Proistosescu C, Kang S M, Xie S-P, Kim D, McGregor S, Zhang W and Zhao S 2018 Polar amplification dominated by local forcing and feedbacks *Nat. Clim. Change* **8** 1076–81

[12] Bintanja R, Graversen R and Hazeleger W 2011 Arctic winter warming amplified by the thermal inversion and consequent low infrared cooling to space *Nat. Geosci.* **4** 758–61

[13] Pithan F and Mauritsen T 2014 Arctic amplification dominated by temperature feedbacks in contemporary climate models *Nat. Geosci.* **7** 181–4

[14] Schweiger A J, Lindsay R W, Vavrus S and Francis J A 2008 Relationships between Arctic sea ice and clouds during autumn *J. Clim.* **21** 4799–810

[15] Kay J E and Gettelman A 2009 Cloud influence on and response to seasonal Arctic sea ice loss *J. Geophys. Res. Atmos.* **114** D18204

[16] Winton M 2006 Amplified Arctic climate change: what does surface albedo feedback have to do with it? *Geophys. Res. Lett.* **33** L03701

[17] Ding Q, Wallace J M, Battisti D S, Steig E J, Gallant A J, Kim H-J and Geng L 2014 Tropical forcing of the recent rapid Arctic warming in northeastern Canada and Greenland *Nature* **509** 209–12

[18] Laîné A, Yoshimori M and Abe-Ouchi A 2016 Surface Arctic amplification factors in CMIP5 models: land and oceanic surfaces and seasonality *J. Clim.* **29** 3297–316

[19] Perlwitz J, Hoerling M and Dole R 2015 Arctic tropospheric warming: causes and linkages to lower latitudes *J. Clim.* **28** 2154–67

[20] Woods C and Caballero R 2016 The role of moist intrusions in winter Arctic warming and sea ice decline *J. Clim.* **29** 4473–85

[21] Francis J A and Vavrus S J 2012 Evidence linking Arctic amplification to extreme weather in mid-latitudes *Geophys. Res. Lett.* **39** L06801

[22] Tang Q, Zhang X, Yang X and Francis J A 2013 Cold winter extremes in northern continents linked to Arctic sea ice loss *Environ. Res. Lett.* **8** 014036

[23] Walsh J E 2014 Intensified warming of the Arctic: causes and impacts on middle latitudes *Glob. Planet. Change* **117** 52–63

[24] Overland J E, Wood K R and Wang M 2011 Warm Arctic—cold continents: climate impacts of the newly open Arctic Sea *Polar Res.* **30** 15787

[25] Cohen J, Jones J, Furtado J C and Tziperman E 2013 Warm Arctic, cold continents: a common pattern related to Arctic sea ice melt, snow advance, and extreme winter weather *Oceanography* **26** 150–60

[26] Cohen J L, Furtado J C, Barlow M A, Alexeev V A and Cherry J E 2012 Arctic warming, increasing snow cover and widespread boreal winter cooling *Environ. Res. Lett.* **7** 014007
[27] Honda M, Inoue J and Yamane S 2009 Influence of low Arctic sea-ice minima on anomalously cold Eurasian winters *Geophys. Res. Lett.* **36** L08707
[28] Mori M, Watanabe M, Shiogama H, Inoue J and Kimoto M 2014 Robust Arctic sea-ice influence on the frequent Eurasian cold winters in past decades *Nat. Geosci.* **7** 869–73
[29] Kug J-S, Jeong J-H, Jang Y-S, Kim B-M, Folland C K, Min S-K and Son S-W 2015 Two distinct influences of Arctic warming on cold winters over North America and East Asia *Nat. Geosci.* **8** 759–62
[30] Kim B-M, Son S-W, Min S-K, Jeong J-H, Kim S-J, Zhang X, Shim T and Yoon J-H 2014 Weakening of the stratospheric polar vortex by Arctic sea-ice loss *Nat. Commun.* **5** 1–8
[31] Hoshi K, Ukita J, Honda M, Nakamura T, Yamazaki K, Miyoshi Y and Jaiser R 2019 Weak stratospheric polar vortex events modulated by the Arctic sea-ice loss *J. Geophys. Res. Atmos.* **124** 858–69
[32] Yang X-Y, Yuan X and Ting M 2016 Dynamical link between the Barents–Kara sea ice and the Arctic Oscillation *J. Clim.* **29** 5103–22
[33] Zhang J, Tian W, Chipperfield M P, Xie F and Huang J 2016 Persistent shift of the Arctic polar vortex towards the Eurasian continent in recent decades *Nat. Clim. Change* **6** 1094–9
[34] Wu B, Su J and Zhang R 2011 Effects of autumn-winter Arctic sea ice on winter Siberian High *Chin. Sci. Bull.* **56** 3220–8
[35] Luo D, Xiao Y, Yao Y, Dai A, Simmonds I and Franzke C L 2016 Impact of Ural blocking on winter warm Arctic–cold Eurasian anomalies. Part I: blocking-induced amplification *J. Clim.* **29** 3925–47
[36] Blackport R and Screen J A 2020 Insignificant effect of Arctic amplification on the amplitude of midlatitude atmospheric waves *Sci. Adv.* **6** eaay2880
[37] Liang Y-C, Frankignoul C, Kwon Y-O, Gastineau G, Manzini E, Danabasoglu G, Suo L, Yeager S, Gao Y and Attema J J 2021 Impacts of Arctic sea ice on cold season atmospheric variability and trends estimated from observations and a multimodel large ensemble *J. Clim.* **34** 8419–43
[38] Wang S and Chen W 2022 Impact of internal variability on recent opposite trends in wintertime temperature over the Barents–Kara Seas and central Eurasia *Clim. Dyn.* **58** 2941–56
[39] Blackport R, Screen J A, van der Wiel K and Bintanja R 2019 Minimal influence of reduced Arctic sea ice on coincident cold winters in mid-latitudes *Nat. Clim. Change* **9** 697–704
[40] Dai A and Song M 2020 Little influence of Arctic amplification on mid-latitude climate *Nat. Clim. Change* **10** 231–7
[41] McCusker K E, Fyfe J C and Sigmond M 2016 Twenty-five winters of unexpected Eurasian cooling unlikely due to Arctic sea-ice loss *Nat. Geosci.* **9** 838–42
[42] Sigmond M and Fyfe J C 2016 Tropical Pacific impacts on cooling North American winters *Nat. Clim. Change* **6** 970–4
[43] Smith D M, Eade R, Andrews M, Ayres H, Clark A, Chripko S, Deser C, Dunstone N, García-Serrano J and Gastineau G 2022 Robust but weak winter atmospheric circulation response to future Arctic sea ice loss *Nat. Commun.* **13** 1–15
[44] He S, Xu X, Furevik T and Gao Y 2020 Eurasian cooling linked to the vertical distribution of Arctic warming *Geophys. Res. Lett.* **47** e2020GL087212
[45] Mori M, Kosaka Y, Watanabe M, Nakamura H and Kimoto M 2019 A reconciled estimate of the influence of Arctic sea-ice loss on recent Eurasian cooling *Nat. Clim. Change* **9** 123–9
[46] Blackport R and Screen J A 2020 Weakened evidence for mid-latitude impacts of Arctic warming *Nat. Clim. Change* **10** 1065–6
[47] Blackport R and Screen J A 2021 Observed statistical connections overestimate the causal effects of arctic sea ice changes on midlatitude winter climate *J. Clim.* **34** 3021–38
[48] Cohen J, Pfeiffer K and Francis J A 2018 Warm Arctic episodes linked with increased frequency of extreme winter weather in the United States *Nat. Commun.* **9** 1–12
[49] Kretschmer M, Coumou D, Agel L, Barlow M, Tziperman E and Cohen J 2018 More-persistent weak stratospheric polar vortex states linked to cold extremes *Bull. Am. Meteorol. Soc.* **99** 49–60
[50] Cohen J, Agel L, Barlow M, Garfinkel C I and White I 2021 Linking Arctic variability and change with extreme winter weather in the United States *Science* **373** 1116–21
[51] Lee S, Furtado J and Charlton-Perez A 2019 Wintertime North American weather regimes and the Arctic stratospheric polar vortex *Geophys. Res. Lett.* **46** 14892–900
[52] Zhang P, Wu Y, Chen G and Yu Y 2020 North American cold events following sudden stratospheric warming in the presence of low Barents–Kara Sea sea ice *Environ. Res. Lett.* **15** 124017
[53] Ma S and Zhu C 2020 Opposing trends of winter cold extremes over Eastern Eurasia and North America under recent Arctic warming *Adv. Atmos. Sci.* **37** 1417–34
[54] Sung M-K, Son S-W, Yoo C, Hwang J and An S-I 2021 Seesawing of winter temperature extremes between East Asia and North America *J. Clim.* **34** 4423–34
[55] Liu Z, Tang Y, Jian Z, Poulsen C J, Welker J M and Bowen G J 2017 Pacific North American circulation pattern links external forcing and North American hydroclimatic change over the past millennium *Proc. Natl Acad. Sci.* **114** 3340–5
[56] Nigam S, Thomas N P, Ruiz-Barradas A and Weaver S J 2017 Striking seasonality in the secular warming of the northern continents: structure and mechanisms *J. Clim.* **30** 6521–41
[57] Rayner N, Parker D E, Horton E, Folland C K, Alexander L V, Rowell D, Kent E C and Kaplan A 2003 Global analyses of sea surface temperature, sea ice, and night marine air temperature since the late nineteenth century *J. Geophys. Res. Atmos.* **108** D14
[58] Gelaro R, McCarty W, Suárez M J, Todling R, Molod A, Takacs L, Randles C A, Darmenov A, Bosilovich M G and Reichle R 2017 The modern-era retrospective analysis for research and applications, version 2 (MERRA-2) *J. Clim.* **30** 5419–54
[59] Hersbach H, Bell B, Berrisford P, Hirahara S, Horányi A, Muñoz-Sabater J, Nicolas J, Peubey C, Radu R and Schepers D 2020 The ERA5 global reanalysis *Q. J. R. Meteorol. Soc.* **146** 1999–2049
[60] Kobayashi S, Ota Y, Harada Y, Ebita A, Moriya M, Onoda H, Onogi K, Kamahori H, Kobayashi C and Endo H 2015 The JRA-55 reanalysis: general specifications and basic characteristics *J. Meteorol. Soc.* **93** 5–48
[61] Menne M J, Williams C N, Gleason B E, Rennie J J and Lawrimore J H 2018 The global historical climatology network monthly temperature dataset, version 4 *J. Clim.* **31** 9835–54
[62] Gocic M and Trajkovic S 2013 Analysis of changes in meteorological variables using Mann-Kendall and Sen's slope estimator statistical tests in Serbia *Glob. Planet. Change* **100** 172–82
[63] Hannachi A, Jolliffe I T and Stephenson D B 2007 Empirical orthogonal functions and related techniques in atmospheric science: a review *Int. J. Climatol.* **27** 1119–52
[64] Bretherton C S, Smith C and Wallace J M 1992 An intercomparison of methods for finding coupled patterns in climate data *J. Clim.* **5** 541–60
[65] Wallace J M, Fu Q, Smoliak B V, Lin P and Johanson C M 2012 Simulated versus observed patterns of warming over the extratropical Northern Hemisphere continents during the cold season *Proc. Natl Acad. Sci.* **109** 14337–42
[66] Simon A, Frankignoul C, Gastineau G and Kwon Y-O 2020 An observational estimate of the direct response of the

cold-season atmospheric circulation to the Arctic Sea Ice Loss *J. Clim.* **33** 3863–82
[67] Peings Y 2019 Ural blocking as a driver of early-winter stratospheric warmings *Geophys. Res. Lett.* **46** 5460–8
[68] Luo B, Wu L, Luo D, Dai A and Simmonds I 2019 The winter midlatitude-Arctic interaction: effects of North Atlantic SST and high-latitude blocking on Arctic sea ice and Eurasian cooling *Clim. Dyn.* **52** 2981–3004
[69] Petoukhov V and Semenov V A 2010 A link between reduced Barents–Kara sea ice and cold winter extremes over northern continents *J. Geophys. Res. Atmos.* **115** D21111
[70] Smedsrud L H, Esau I, Ingvaldsen R B, Eldevik T, Haugan P M, Li C, Lien V S, Olsen A, Omar A M and Otterå O H 2013 The role of the Barents Sea in the Arctic climate system *Rev. Geophys.* **51** 415–49
[71] Chen H W, Alley R B and Zhang F 2016 Interannual Arctic sea ice variability and associated winter weather patterns: a regional perspective for 1979–2014 *J. Geophys. Res. Atmos.* **121** 14–433
[72] Sato K, Inoue J and Watanabe M 2014 Influence of the Gulf Stream on the Barents Sea ice retreat and Eurasian coldness during early winter *Environ. Res. Lett.* **9** 084009
[73] Shu Q, Wang Q, Song Z and Qiao F 2021 The poleward enhanced Arctic Ocean cooling machine in a warming climate *Nat. Commun.* **12** 1–9
[74] Outten S and Esau I 2012 A link between Arctic sea ice and recent cooling trends over Eurasia *Clim. Change* **110** 1069–75
[75] Li C, Stevens B and Marotzke J 2015 Eurasian winter cooling in the warming hiatus of 1998–2012 *Geophys. Res. Lett.* **42** 8131–9
[76] Wang Y, Zhang G J, Gong P, Dickinson R E, Fu R, Li X, Yang J, Liu S, He Y and Li L 2021 Winter warming in North America induced by urbanization in China *Geophys. Res. Lett.* **48** e2021GL095465
[77] Sun L, Perlwitz J and Hoerling M 2016 What caused the recent "Warm Arctic, Cold Continents" trend pattern in winter temperatures? *Geophys. Res. Lett.* **43** 5345–52
[78] Chen H W, Zhang F and Alley R B 2016 The robustness of midlatitude weather pattern changes due to Arctic sea ice loss *J. Clim.* **29** 7831–49
[79] Screen J A, Deser C, Simmonds I and Tomas R 2014 Atmospheric impacts of Arctic sea-ice loss, 1979–2009: separating forced change from atmospheric internal variability *Clim. Dyn.* **43** 333–44
[80] Ogawa F, Keenlyside N, Gao Y, Koenigk T, Yang S, Suo L, Wang T, Gastineau G, Nakamura T and Cheung H N 2018 Evaluating impacts of recent Arctic sea ice loss on the Northern Hemisphere winter climate change *Geophys. Res. Lett.* **45** 3255–63
[81] Yao Y, Luo D, Dai A and Simmonds I 2017 Increased quasi stationarity and persistence of winter Ural blocking and Eurasian extreme cold events in response to Arctic warming. Part I: insights from observational analyses *J. Clim.* **30** 3549–68
[82] Plumb R A 1985 On the three-dimensional propagation of stationary waves *J. Atmos. Sci.* **42** 217–29
[83] Luo D, Chen X, Overland J, Simmonds I, Wu Y and Zhang P 2019 Weakened potential vorticity barrier linked to recent winter Arctic sea ice loss and midlatitude cold extremes *J. Clim.* **32** 4235–61